water

MDPI

Article

Estimations of Crop Losses Due to Flood Using Multiple Sources of Information and Models: The Case Study of the Panaro River

Beatrice Monteleone [1,*], Riccardo Giusti [1], Andrea Magnini [2], Marcello Arosio [1], Alessio Domeneghetti [2], Iolanda Borzì [3], Natasha Petruccelli [2], Attilio Castellarin [2], Brunella Bonaccorso [3] and Mario L. V. Martina [1]

[1] Department of Sciences, Technologies and Society, University School for Advanced Studies of Pavia, 27100 Pavia, Italy; riccardo.giusti@iusspavia.it (R.G.); marcello.arosio@iusspavia.it (M.A.); mario.martina@iusspavia.it (M.L.V.M.)
[2] Department of Civil, Chemical, Environmental and Materials Engineering (DICAM), University of Bologna, 40126 Bologna, Italy; andrea.magnini@unibo.it (A.M.); alessio.domeneghetti@unibo.it (A.D.); natasha.petruccelli@unibo.it (N.P.); lattilio.castellarin@unibo.it (A.C.)
[3] Department of Engineering, University of Messina, Villaggio Sant'Agata, 98166 Messina, Italy; iolanda.borzi@unime.it (I.B.); brunella.bonaccorso@unime.it (B.B.)
* Correspondence: beatrice.monteleone@iusspavia.it

Abstract: Floods and droughts are the events that most threaten crop production; however, the impact of floods on crops is still not fully understood and often under-reported. Nowadays, multiple sources of information and approaches support the estimation of agricultural losses due to floods. This study aims to understand the differences in agricultural loss estimates provided by two conceptually different approaches (crop models and expert-based models), evaluating their sensitivity to flood hazard inputs. We investigated the challenges in flood agricultural loss assessments referring to a case study for which, in addition to model simulations, information from surveys and on-site inspections were available. Two crop models (APSIM and WOFOST) and the expert-based model AGRIDE-c were applied to evaluate agricultural yield losses after the flood event of the Panaro River (Emilia-Romagna, Northern Italy) that took place on the 6 December 2020. Two modelling tools were used to reproduce the event: the hydraulic model HEC-RAS and the image-based tool FwDET. Additionally, surveys among local farmers were conducted in the aftermath of the event to evaluate the flood features (water depth, extent and duration) and crop losses. The main findings of the study are that APSIM and WOFOST provide similar estimates of yield losses, while AGRIDE-c tends to underestimate yield losses when the losses over the entire study area are evaluated. The choice of the flood simulation technique does not influence the loss estimation since the difference between the yield loss estimates retrieved from the same model initialized with HEC-RAS or FwDET was always lower than 2%. Information retrieved from the surveys was not sufficient to validate the damage estimates provided by the models but could be used to derive a qualitative picture of the event. Therefore, further research is needed to understand how to effectively incorporate this kind of information in agricultural loss estimation.

Keywords: flood risk assessment; crop yield losses; comparative analysis; crop models; expert-based models

Citation: Monteleone, B.; Giusti, R.; Magnini, A.; Arosio, M.; Domeneghetti, A.; Borzì, I.; Petruccelli, N.; Castellarin, A.; Bonaccorso, B.; Martina, M.L.V. Estimations of Crop Losses Due to Flood Using Multiple Sources of Information and Models: The Case Study of the Panaro River. *Water* **2023**, *15*, 1980. https://doi.org/10.3390/w15111980

Academic Editor: Guido D'Urso

Received: 17 March 2023
Revised: 16 May 2023
Accepted: 18 May 2023
Published: 23 May 2023

1. Introduction

The agricultural sector is traditionally highly vulnerable to natural disasters, given its reliance on favourable weather conditions. From 2008 to 2018, agriculture (crops, livestock, fisheries, forestry and aquaculture) absorbed 26% of the impacts caused by medium- to large-scale natural disasters [1]. Floods and droughts are the most common events that threaten agricultural production. Drought is responsible for around 34% of crop and

livestock production losses, with flood being the second most serious disaster, bearing 19% of the total production losses in low- and middle-income countries [2].

The impacts of flood on agriculture are still not fully understood and are often underreported [3]. This can be linked to the perceived minor importance of the agricultural sector when compared to industrial or residential ones: in cases of similar exposure, the damage associated with the former sector is comparatively lower than the others [4]. Furthermore, the common approach of assessing agricultural impacts aggregated at the national level does not allow for the inclusion of localized impacts that are typical of floods [5].

Crop susceptibility to floods is strictly linked with plant development and flood characteristics [6]. Agricultural crop losses are strongly influenced by the season and the period of the year [7] and depend on the flood water depth, its duration and the flow velocity.

The latter (water depth, flood duration and flow velocity) has been used in multiple studies to develop functions relating one or more of these variables to crop damage, expressed in physical terms (yield losses) or economic terms [8]. For example, [9,10] related water depth with rice yield losses in Asia, while [11] established a link between flood duration and yield losses. The authors of [12] proposed damage surfaces for fruit trees and vegetables relating the crop damage to flow velocity and water depth in a Greek basin, whereas [4] reviewed studies relating the flood parameters to economic losses experienced by farmers because of the inundations.

Crop damage functions have been developed predominantly starting from observations of the reported crop losses associated with past flood events of various magnitudes (see [13,14]) or, rarely, on field experiments specifically carried out, as in [15]. While field experiments require a lot of effort, the collection and harmonization of data and expert knowledge on flood damage to crops are recommended to derive the relationships between yield losses and flood parameters, as evidenced in [4].

Expert-based models, i.e., those based on the opinion of experts, or qualitative models based on the best information available from the literature, rely on the knowledge of farmers, agronomists, etc., to assess crop damage due to a flood event with specific characteristics. Some examples include (1) flooddam.agri, which evaluates the flood impacts on the agricultural sector through variation of the added value through the production process, this model has been applied in France [16]; (2) AGRIDE-c (Agriculture Damage Model for Crops) [17], a model evaluating cereal and forage losses due to flood based on water depth and flood duration in the context of Northern Italy; (3) a procedure to assess the monthly damage for a wide variety of agricultural schemes and crops, which was tested in a German case study (flood of river Elbe) [18].

More recently, models capable of reproducing crop yield losses due to floods have been applied to derive the relationships between the yield decrease and flood parameters. An additional component for the APSIM crop model (Agricultural Production System Simulator [19]) was capable of simulating the yield decrease from excess rain or flood events by taking into account the effects of waterlogging on soybean plants [20]. The inclusion of the effects of waterlogging in crop models is crucial to allow their application in agricultural loss estimation since this mechanism is responsible for up to 50% of the yield losses depending on the crop type, the crop growth stage and the water depth [21]. Crop models incorporating the waterlogging mechanism, even if they are unable to simulate other flood-associated mechanisms that cause damage to crops (e.g., crop destruction due to high flow velocity or the decrease in plant yield due to the decrease in the available light in the case of submergence), could be a powerful tool to provide indications on yield losses associated with an event with specific characteristics.

Both crop models and expert-based models show benefits and drawbacks. Crop models are based on biological processes driven by physical variables linked with plant growth but require multiple input variables and need to be tailored to the context of each case study. Expert-based models are instead already tailored to a specific context or location, but their scalability is complex since the expert knowledge on which they are built up is

referred to in the case study, or to the technical, economic and environmental contexts for which they have been developed.

Both approaches require parameters on the water depth, flood extent and duration as the input. Thus, the damage estimation performed with the two methods strictly depends on the hazard simulation. The level of detail required by the hazard simulation is a topic that deserves further exploration, since the selection of a specific methodology depends on the compromise between its accuracy and the data requirement [22]. Nowadays, many different methodologies are available for the reproduction and observation of hazardous variables such as satellite technologies, simplified approaches [23–25], etc. The adoption of hydraulic models represents a classic and well-consolidated approach. Hydraulic models of different complexity and structures are in fact available in relation to the scope, offering the opportunity to simulate riverine inundation both at the local and continental (or even global) scale [26,27], reproducing the hydraulic variables required for the direct and indirect flood damage assessment [28]. In addition, given the high availability of remote sensing data, flood extent analysis from satellite images is gaining interest. Remote sensing images, consisting of continuous spatial fields, are extremely useful to obtain observational information on the inundation extent [29]. Although several approaches to estimate flood water depth from remote sensing images are currently available [30,31], its estimation is still affected by uncertainties that may impact the flood loss estimation.

Both the application of hydraulic models and the use of remote sensing images exhibit advantages and disadvantages. Hydraulic models usually provide very detailed information on the water depth, flood velocity and timing of the flood event, but do not supply information on flood duration. In addition, their accuracy is strictly dependent on the quality of the input data and model calibration. Moreover, the time required to run the model varies according to its complexity and the spatial and temporal resolution of the input data. The use of remote sensing images on the other hand, could provide information on the flood extent shortly after the event, thus allowing rapid estimation of the damage and, when multiple images retrieved in the days after the flood are available, could provide useful information on the duration. The main disadvantages of using satellite data lie in the uncertainty of the water depth assessments and the availability of images retrieved following the event.

The assessment of how crop damage estimation varies in relation to the complexity and accuracy of the hazard modelling is an interesting element that deserves evaluation [32].

Therefore, this study applies the expert-based model AGRIDE-c and two crop models (previously mentioned APSIM and the World Food Studies model WOFOST) to assess crop damage due to flood with the following aims:

- understand the differences in the agricultural yield loss estimate retrieved with the two conceptually different damage estimation approaches;
- assess how different inundation modelling approaches (i.e., HEC-RAS 6.1 and the Floodwater Depth Estimation Tool, FwDET v2.0) influence crop loss estimation;
- investigate the challenges and future developments in flood crop damage based on the results obtained for a past event for which multi-source information is available.

The flood event of the Panaro River (Emilia-Romagna, Italy) that took place on the 6 December 2020 was chosen as a case study. The choice of this event was due to multiple factors: Firstly, the flood mostly occurred in an agricultural area and the Emilia-Romagna region reported high agricultural damage [33]. Secondly, the availability of information directly collected by the authors in the aftermath on the flood water depth, duration, extent and agricultural damage. Information on the flood extent was directly retrieved from in situ observations, while agricultural damage was collected from post-event surveys among local farmers. The information collected directly from farmers on crop damage is valuable to consolidate model estimations, as underlined by [4], even if the sample is limited. Thirdly, satellite images acquired the day after the flood and six days after the event were available. This last source of information was used to assess the flood duration, together with frequent updates on the situation in the municipality affected by the flood.

The updates were retrieved from online newspapers and reports from the authorities in charge of managing the emergency.

An innovative element of this study lies in the combination of multiple types of information from different sources, while analysing a flood event, comparison of the information from different sources represents a useful way to assess, at least qualitatively, the quality of information. Furthermore, collecting different kinds of information (such as modelling outputs, satellite images and surveys) provides scientists with a broad perspective on the flood event in its complexity, leading to a more reliable estimation of the agricultural damage produced by flood events.

2. Case Study

As previously mentioned, the case study is the flood event that took place on the 6 December 2020 on the Panaro River (Emilia-Romagna region, Italy; Figure 1).

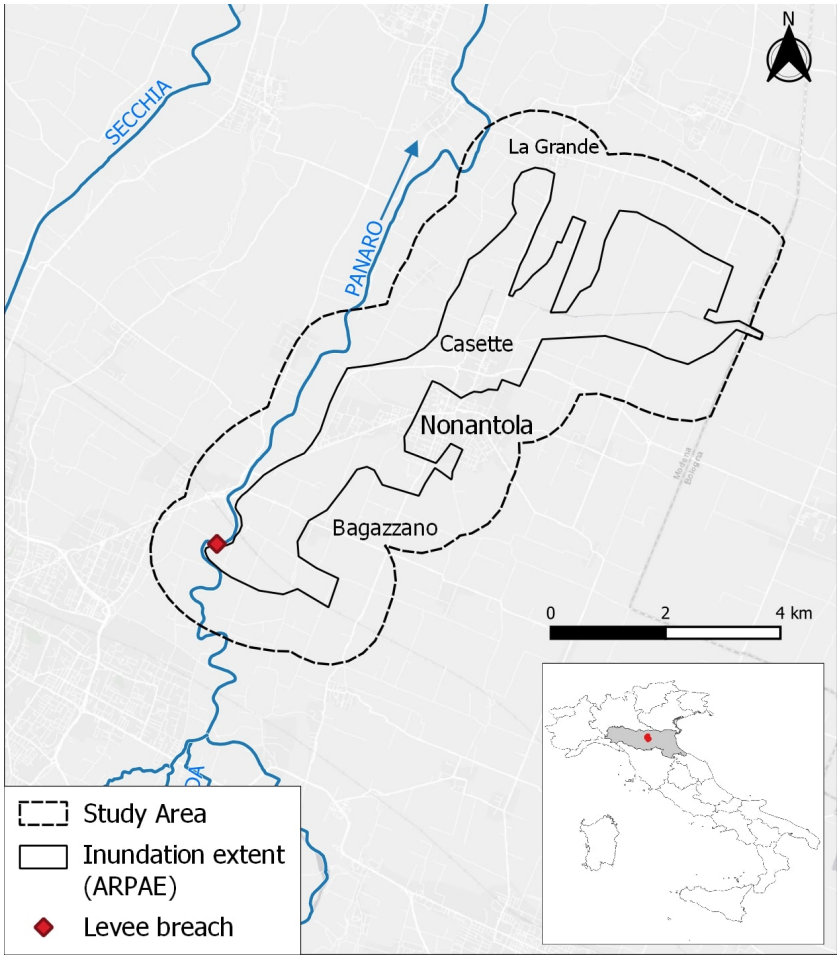

Figure 1. Location of the Emilia-Romagna region in Italy (highlighted in grey), the municipalities affected by the flood event, (Nonantola and Castelfranco Emilia), the case study area and the levee breach on the Panaro river. In addition, the inundation extent determined by the Regional Agency for Environmental Protection of Emilia-Romagna (ARPAE) is reported.

The riverine inundation was due to the formation of a breach in the right levee of the Panaro River, in the municipality of Castelfranco Emilia. The levee breach caused a flood that mostly affected Nonantola, but also had consequences in Castelfranco Emilia. Hydrological reports and technical analyses of the Regional Agency for Environmental Protection of Emilia-Romagna (ARPAE) documented the overall event and the subsequent interventions: the breach reached a maximum length of 80 m, and was repaired approximately 24 h after its formation [33]. The failure of the embankment resulted in a flooded area of

about 15 km^2, mostly in rural areas, but included a minor urban settlement (364 people were evacuated).

ARPAE also reported the inundation extent the day after the event. The selected case study area (dashed line in Figure 1) is thus a buffer of the ARPAE inundation extent, since the authors were aware of flooded areas located outside the ARPAE extent [34].

The flooded area is normally devoted to agriculture. Crops grown in each field within the area of interest ("Study area" in Figure 1) were identified using an open-source dataset provided by the Emilia-Romagna region. The field boundaries were identified through the regional land registry office, the crops grown in the 2020/2021 agricultural season were determined through farmers' yearly declarations on the intended use of each field [35].

The main crops grown in the area affected by the flood event in the 2020/2021 season according to the Geoportale dell'Emilia-Romagna were alfalfa (30.4% of the harvested area), winter wheat (23.67%), sorghum (9.07%) and maize (7.19%) (Figure 2). Other minor crops grown in the area were vineyards (4.67%), pear (4.44%), sugar beet (3.38%) and barley (1.42%). Farmers did not provide declarations regarding crops grown in the remaining part of the harvested area (15.4%) [36].

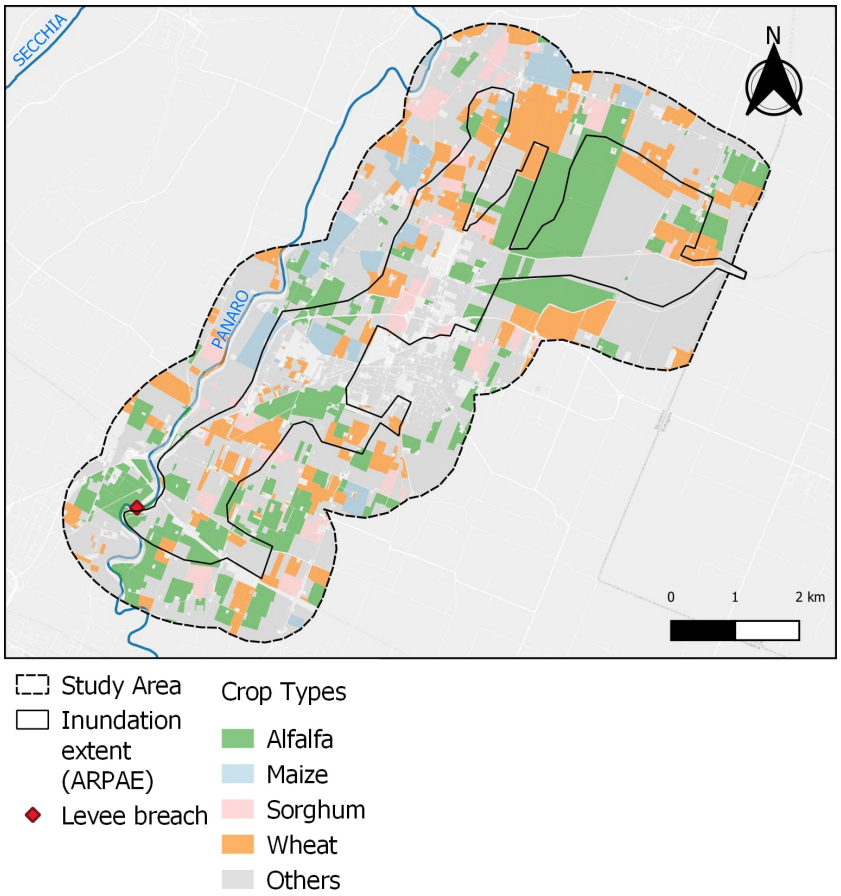

Figure 2. Crops grown in the case study area according to the regional dataset Geoportale dell' Emilia-Romagna.

Information on the crop sowing periods were used to assess which crops were growing at the time of the event and thus impacted by the flood. The sowing periods of the major crops grown in the area are reported in Table 1. At the time of the event, 6 December, only forage, winter crops and orchards were present. In particular, the crops affected by the flood event were alfalfa (a forage that is traditionally sown in spring or autumn, left in the field for three or four years, and cut periodically from May to October), winter wheat, sown between October and November and harvested between June and July, and barley. Alfalfa and winter wheat together accounted for 54% of the considered harvested area;

barley represented only 1.4%. Maize and sorghum, which together represented 16% of the harvested area, are planted in spring and harvested in early autumn; therefore, they were not impacted by the flood.

Table 1. Sowing periods of the main crops grown in the case study area.

Crop Type	Sowing Period	Crop Area (% with Respect to the Total Considered Area)	Reference
Winter wheat	October–November	23.67	[37]
Sorghum	April–May	9.07	[38]
Maize	April–May	7.19	[39]
Alfalfa	Spring or late summer	30.04	[40]

3. Methodology

This study applied the expert-based model AGRIDE-c and the crop models APSIM and WOFOST to estimate crop losses due to the flood event of the Panaro River. Then we evaluated the sensitivity of both models to the methodology used to simulate the hazard by reproducing the flood extent and water depth with the hydraulic model HEC-RAS (v. 6.1) and the remote sensing-based tool FwDET. Flood duration was determined through the use of satellite images and information from reports and updates on the emergency retrieved from online newspapers and reports from local authorities. Finally, the outputs of the crop loss estimations were compared with the the post-event surveys collected by the authors (the questions are reported in Appendix A).

Figure 3 describes the conceptual framework followed in the study, while Table 2 provides a summary of the models used for flood hazard, crop growth and crop damage simulation. Finally, a brief description on how the field surveys were organized and collected is proposed.

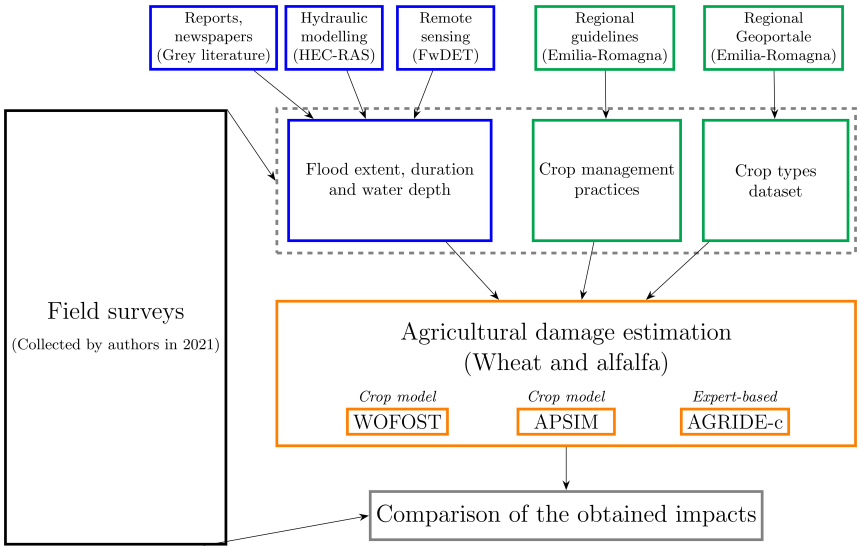

Figure 3. Conceptual methodological framework adopted in this study. The blue boxes contain the inputs related to the flood hazard simulation, the green ones the inputs related with agriculture (management practices and crop types), the black box represent the surveys done by the authors, the orange boxes show the tools used in this study, while the grey box displays the obtained results.

Table 2. Models used in this study and their main features.

Model	Model Type	Reference
HEC-RAS	Numerical hydraulic model	[41]
FwDET	Remote sensing and DEM-based inundation water depth calculation tool	[30]
APSIM	Crop model	[19]
WOFOST	Crop model	[42]
AGRIDE-c	Expert-based damage model	[17]

To maintain the structure described in the flowchart, the techniques used to simulate the hazard (i.e., the flood event) are first described, then the methodology to derive the agricultural losses.

3.1. Hazard Estimation

Two techniques for water depth and flood extent simulation were considered in this study: the hydraulic model HEC-RAS and the FwDET tool, providing information on the flood water depth starting from post-event satellite images. In addition, satellites images were exploited to determine the flood duration, together with information from online newspapers and reports from the local authorities.

3.1.1. Flood Extent and Water Depth Estimation from HEC-RAS

HEC-RAS (from v. 6.x on) is a coupled 1D–2D hydraulic model [41] that performs steady and unsteady flow river hydraulic calculations to solve the mono- and bi-dimensional De Saint Venant equations [43]. In this application, the 1D model was used to simulate the flow routing along the Panaro River, whose geometry was reproduced taking advantage of the Digital Elevation Model (DEM) of the Emilia-Romagna region (LiDAR-based, 1 m resolution) and in situ measured cross-sections. The calibration of the 1D model has been performed considering a significant past flood event (i.e., 2009 event, for which the discharge and water level series are available from few gauging stations, together with high-water marks surveyed after the flood at several river cross-sections). The 1D model was used to reproduce the hydraulic loads (flow velocity, water depths, inundation duration, etc.) at river cross-sections where the levee failure occurred. The upstream boundary conditions adopted for simulation of the flood event refer to discharge series observed at the upstream gauging station, while a normal flowing condition was imposed as a downstream boundary condition. A 2D model, fully coupled with the 1D model, was used to reproduce the inundation dynamics within the flood-prone area. Particular attention was paid to correcting the elevation values of the LiDAR in order to adequately represent buildings, minor river networks, hydraulic structures and road embankments that significantly affected the water dynamics. This resulted in a 2D mesh whose resolution varied between 3 and 20 m. Calibration of the 2D model relies on several parameters available about the area: land-use from the Corine Land Cover dataset [44], satellite data acquired during the event, and pictures taken in situ by citizens and local authorities. Once properly set up, the coupled 1D–2D model provided the flood parameter values necessary for damage estimation, such as flood extent, water depth, velocity and time of arrival.

3.1.2. Water Depth Estimation from FwDET

The extent of the flooded area the day after the levee collapse has been documented by different sources (e.g., remote sensing, in situ surveys, visual testimony) that are listed in a detailed report by the Technical-Scientific Commission for the evaluation of the event [45]. The most precise information came from remote sensing images acquired by the COSMO SkyMed satellite, owned by the Italian Spatial Agency [46], about 24 h after the levee breach. The COSMO SkyMed images were used by the Regional Agency for Environmental Protection of Emilia-Romagna to derive the inundation extent on the 7 December. The Floodwater Depth Estimation Tool (FwDET v2.0), developed by [30], was applied to derive

the water depth, in combination with the DEM of the Emilia-Romagna region. FwDET v2.0 was developed to exploit remote sensing analysis by calculating the water depth solely based on an inundation map with an associated DEM.

3.1.3. Flood Duration Estimation from Satellite Images and Reports

Various sources of information were used to determine the flood duration. Satellite images acquired by COSMO SkyMed on the 7 December 2020 were exploited to identify flooded areas the day after the levee breach. Reports from the local authorities in charge of managing the emergency were used to document areas where water was still present in the days following the levee collapse (8–13 December). Finally, the Copernicus Emergency Management Service took advantage of the satellite images acquired by Geo-Eye-1 on the 13 December to identify areas where water was present one week after the levee breach. It should be noted that the levee collapse caused the inundation of the right side of the Panaro River while the left side was flooded because of intense precipitation occurring during the 4 and 10 December [34]. In this study, the areas located on the left side of the river were excluded from the analysis since the eventual presence of water there was not related to the levee collapse. Table 3 summarizes the sources of information used to determine the flood duration.

Table 3. Flooded areas in the days after the levee collapse.

Day	Flooded Areas	Reference
7 December 2020	Castelfranco Emilia, Nonantola, Frazione La Grande, Bagazzano, Gaggio, areas from Torrazzuolo to Navicello	[47]
8 December 2020	Bagazzano, areas near the levee breach, areas from Torrazzuolo to Navicello, Frazione La Grande, Frazione Casette	[34,48]
9 December 2020	Via Caselle, collettore Bosca, Frazione La Grande, Frazione Casette	[34,49]
10 December 2020	Frazione Casette, Frazione La Grande	[50]
11 December 2020	Via Pasolini	[51]
13 December 2020	Sparse areas	[52]

3.2. Agricultural Losses Estimation

Agricultural losses at the field scale were estimated through the use of crop models and expert-based models.

3.2.1. Field-Scale Estimation through Crop Models

Two crop models were applied to evaluate the crop losses at the field scale: APSIM and WOFOST. Both were selected among the available crop models since they are capable of reproducing the effects of water excess and waterlogging on crops [53]. As inputs, both models require crop management practices information, soil texture class and weather parameters.

The required crop management practices for the two crop models are slightly different. Besides the crop type and sowing date or sowing window, necessary for both the models, APSIM requires additional information such as sowing density, sowing depth and row spacing [54].

The soil texture, classified according to the method proposed by the United States Department of Agriculture [55], was retrieved from the SoilGrids dataset [56]. In the present case, the considered area has a loam soil.

Concerning the weather parameters, the daily maximum, minimum and average temperature, rainfall and solar radiation are mandatory. In addition, WOFOST requires the daily wind speed and vapour pressure deficit. All the weather data were retrieved from the automatic station of Castelfranco Emilia from the 1 August 2020 to 31 August 2021 [47]. Table 4 provides a summary of the data used to initialize both crop models.

Table 4. Summary of the data used to run the APSIM and WOFOST crop models.

Component	Type	Temporal Resolution	APSIM	WOFOST	Source
Weather	Rainfall	Daily	X	X	[47]
	Average temperature	Daily	X	X	[47]
	Minimum temperature	Daily	X	X	[47]
	Maximum temperature	Daily	X	X	[47]
	Solar radiation	Daily	X	X	[47]
	Wind speed	Daily		X	[47]
	Vapour pressure deficit	Daily		X	[47]
Soil	Texture	–	X	X	[56]
Crop management	Crop type	Yearly	X	X	[36]
	Sowing window	Yearly	X	X	[37]
	Sowing depth	Yearly	X		[37]
	Row spacing	Yearly	X		[37]
	Sowing density	Yearly	X		[37]

The crop models were calibrated and validated against observed yield data for the Modena province, derived from the Italian National Institute of Statistics [57]. Further details on the crop model calibration and validation are described in Appendix B.

The calibrated crop models were applied to compute the yield Y, a function of multiple parameters:

$$Y = f(D, PAR, f_s, crop\ parameters) \quad (1)$$

where D is the day length, PAR is the photosynthetically absorbed radiation, and f_s is a stress factor, while the crop-specific parameters are listed in Table 4 under "crop management". The stress factor f_s is expressed as:

$$f_s = min(f_T, f_N, f_O) \quad (2)$$

in which f_T, f_N, and f_O are the temperature, nitrogen and oxygen stress factors, respectively. All the factors range from 0 to 1, with 0 meaning the crop is experiencing the maximum possible stress and 1 meaning there is no stress. Thus, f_s ranges from 0 to 1 too [54].

APSIM and WOFOST are used to retrieve the potential yield Y_P, which is the yield in the absence of any crop stress [58], $f_s = 1$, and the reduced yield Y_R, which is the yield in the presence of a flood event, i.e., accounting for waterlogging. In this latter case we assumed $f_T = f_N = 1$; thus, there is no stress due to temperature or nitrogen deficiency present, only the oxygen stress due to waterlogging, f_O, is considered. As already stated, the crop models only capture part of the crop damage, given the fact they are incapable of simulating the effects of other damaging mechanisms, such as physical damage due to high flow velocity and the decrease in available light due to crop submergence.

The impact of the flood on crop yield was simulated via the introduction of an irrigation component. The amount of irrigation applied is progressive. The relationship between the amount of water and the yield reduction was used to derive the damage functions applied in the case study area to derive the yield losses in each of the study fields.

3.2.2. Field-Scale Losses Estimation through Expert-Based Models

In the present work, AGRIDE-c [17], a conceptual model to estimate the expected flood damage to crops, was applied since it has been specifically designed for Northern Italy. The model requires several inputs specific for each crop type, as well as the adopted management practices and the flood characteristics. In particular, the following data must be provided:

- Crop type;
- Average crop yield (between 2016 and 2020 derived from [57] equivalent to the crop models' potential yield Y_P);
- Flood duration;

- Flood depth;
- Crop growth stage at the time of the flood event.

Once the data are inserted into the model, it provides the reduced yield Y_R in each field based on the damage functions described in [59].

3.2.3. Overall Agricultural Losses

Once $Y_{P,i}$ and $Y_{R,i}$ are defined for each field i for the considered crops, the yield loss $Y_{L,i}$ is computed as:

$$Y_{L,i} = 100 - (Y_{R,i}/Y_{P,i} \times 100) \quad (3)$$

where $Y_{R,i}$ depends on the water depth on the field i. The overall loss in the study area can then be derived as:

$$Y_L = \sum_{i}^{N} Y_{L,i} \quad (4)$$

where N is the total number of fields considered in the study area where a specific crop is grown.

3.3. Field Surveys

In the aftermath of the event, farmers within the area affected by the flood were interviewed to retrieve information on the flood's characteristics, water depth and damage experienced (the surveys' structure is reported in Appendix A).

In total, ten farmers answered the questionnaire, with the majority of them owning more fields and answering for all of them. Farmers indicated the average flood duration, i.e., the amount of time (in days or hours) during which the fields remained flooded, the water depth, and the percentage of their fields that were flooded. In addition, they indicated the field location, cultivated crop, management practices, expected crop yield, crop growth stage at the time of the flood and the cost sustained for crop maintenance until the flood. Figure 4 shows the location of the fields and the cultivated crops for which questionnaires were conducted.

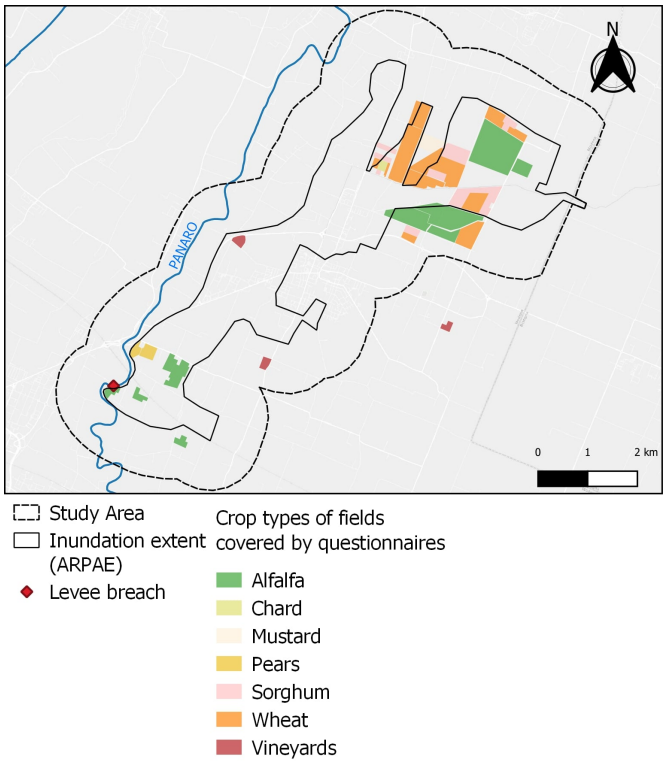

Figure 4. Fieldsand crop type, for which questionnaires were collected.

4. Results

4.1. Inputs for Agricultural Loss Estimation: Data and Information Obtained from Multiple Approaches

The considered case study was analysed from different perspectives. Various information from multiple sources was considered in an attempt to provide a reliable estimation of agricultural losses.

At first, the hazard maps obtained from both the hydraulic model HEC-RAS and the FwDET tool are shown since the evaluation of the agricultural losses was strictly based on the flood extent and water depth simulation when the crop models were applied.

Both tools used the Emilia-Romagna region DEM as the foundation. The flood simulation results performed with HEC-RAS and FwDET are expressed in terms of maps of the overall inundation extent and maximum water depth at each location. Figures 5 and 6 report the overall maximum water depths obtained from the hydraulic model (blue scale colours) and computed through the FwDET tool, respectively.

In addition, in situ measurements, evidenced in Figure 5a,b, were retrieved by the authors six weeks after the flood event, exploiting the fact that flood events are characterized by turbid water that comes into contact with human-made objects, such as buildings, and leave a film called the "mud line". The mud line is recognized as the "high-water mark" [60]. Mud lines on hard surfaces leave better-quality water marks, especially when created by low-velocity water fluxes, lasting for many weeks if undisturbed. High-water marks on residential buildings were measured, geolocalized and photographed. Most of the surveyed buildings have brick walls, where the mud lines were still visible six weeks after the event.

The flood duration over the study area, determined through the information sources listed in Table 3, is reported in Figure 7. Some areas outside the ARPAE inundation extent were flooded, as evidenced by in situ inspections which showed the presence of water in Mavora (Figure 5a), and by the online press, reporting flooded areas in Bagazzano and Frazione La Grande. The maximum flood duration was eight days.

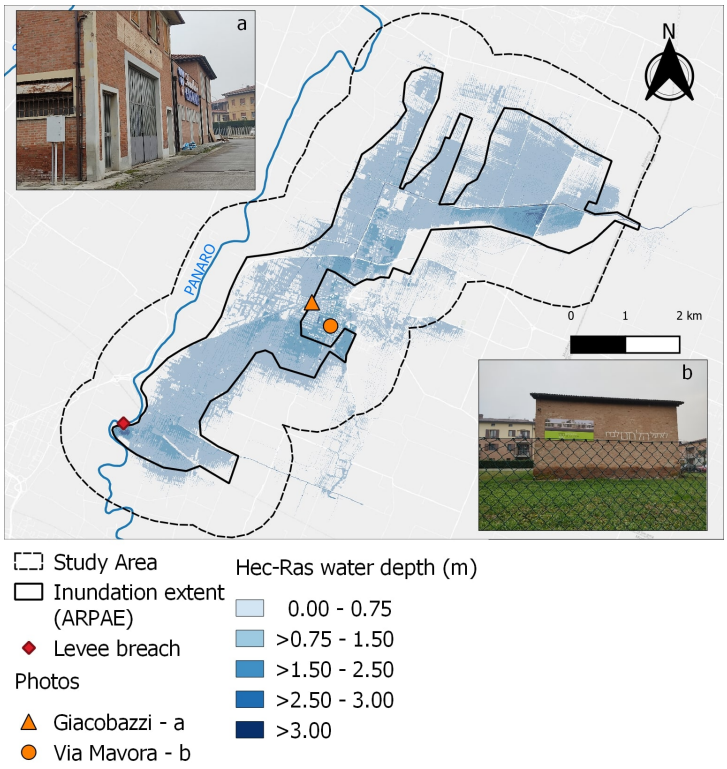

Figure 5. Flood extent and water depth obtained from the hazard simulation performed by HEC-RAS. Panels a and b shows the mud lines on bulidings in Giacobazzi (**a**) and Via Mavora (**b**).

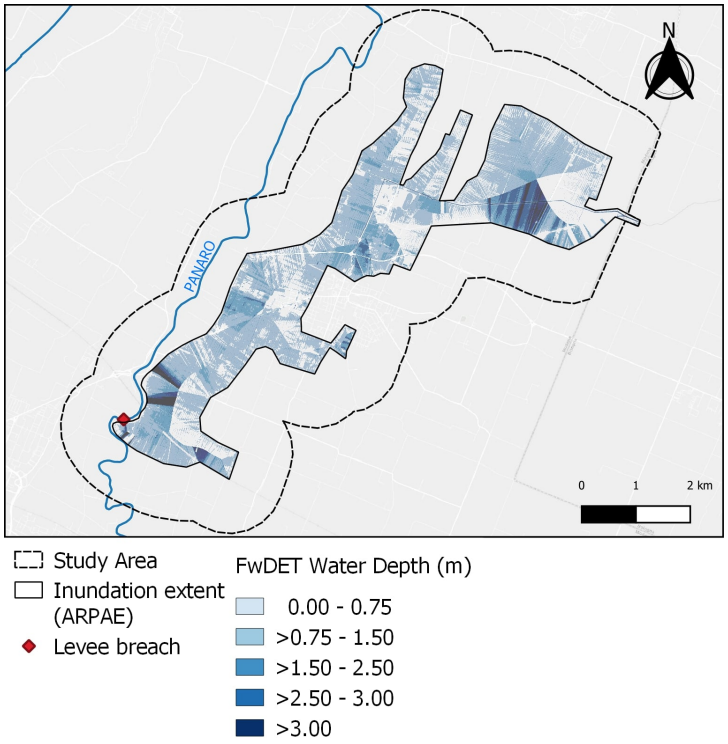

Figure 6. Water depth obtained from FwDET v.2.0. Flood extent in this case was derived from the inundation extent estimated by ARPAE based on the satellite images acquired by COSMO SkyMed 24 h after the event.

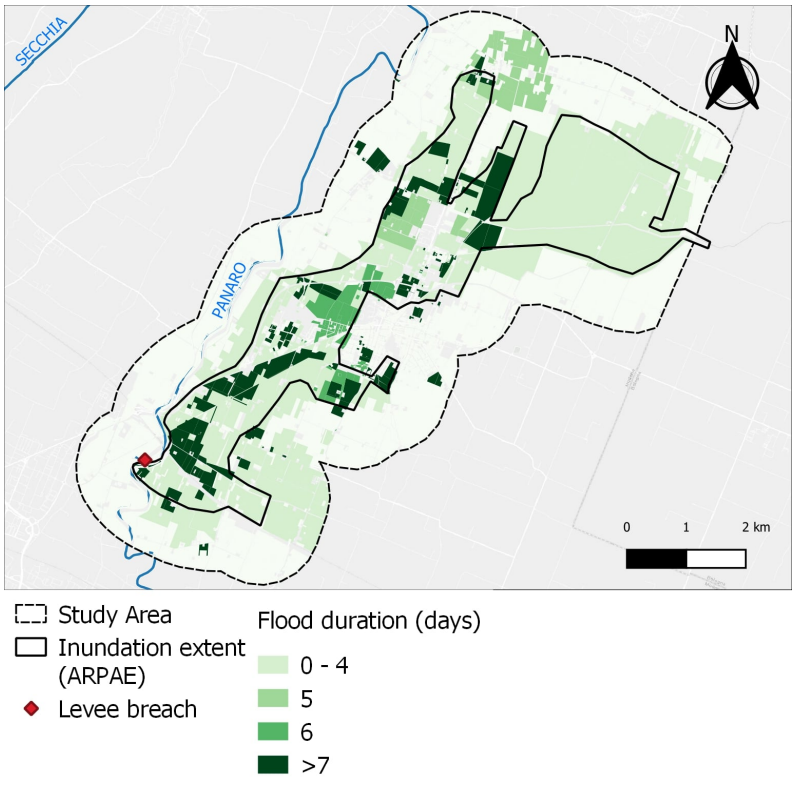

Figure 7. Flood duration in the study area as derived from the sources listed in Table 3. The choice of duration ranges is linked with the winter wheat damage values reported in AGRIDE-c for the "three-leaf stage".

Field surveys also provided information on the flood features. The maximum reconstructed water depth according to the farmers' interviews is shown in Figure 8a. The majority of farmers reported a maximum water depth of 1 m, while farmers with fields close to the levee breach reported water depths around 1.5 m. The majority of the interviewed farmers agreed on a flood duration between 2 and 5 days, with the exception of one, who declared a flood duration of more than 7 days (Figure 8b).

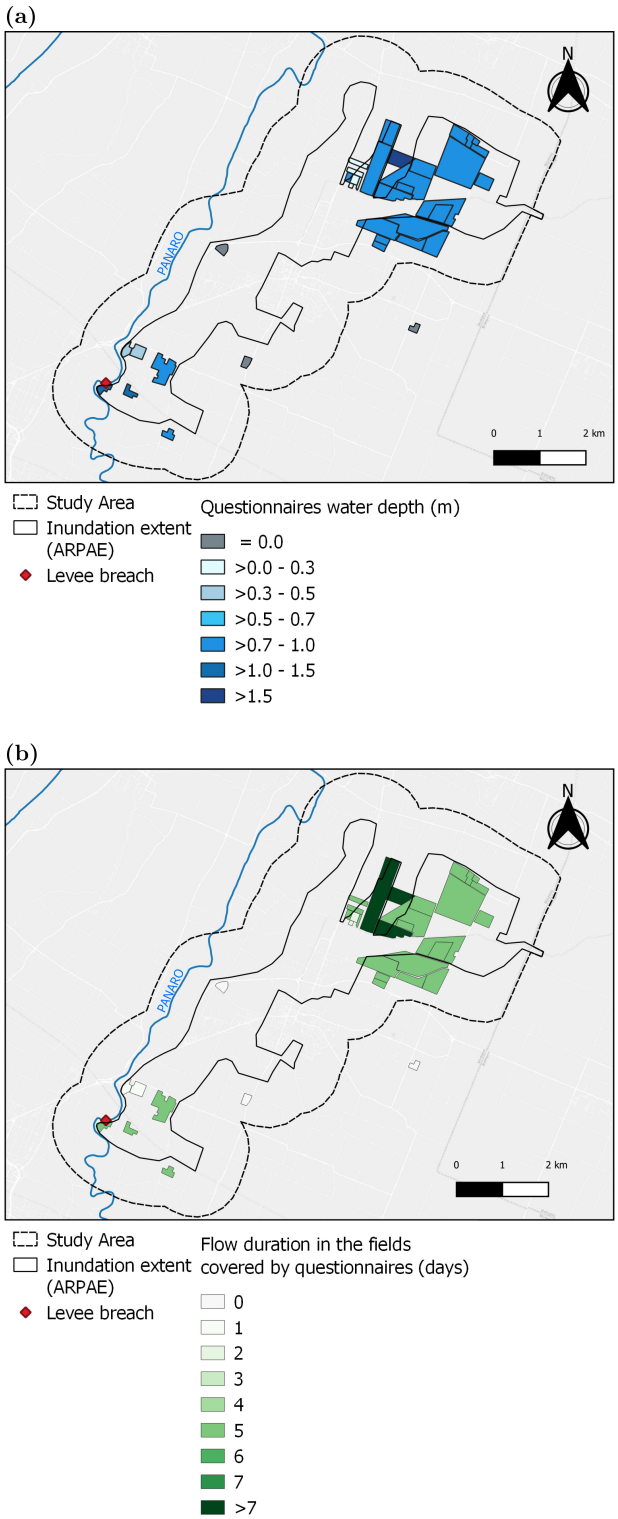

Figure 8. Water depth (**a**) and flood duration (**b**) reported by farmers.

From the same survey, information on the yield losses in the considered fields was retrieved, while farmers cultivating spring crops, such as maize and sorghum, declared no yield losses given the fact the crop was not planted at the time of the flood event (December), farmers cultivating wheat or alfalfa experienced damage. Eleven fields cultivating winter wheat were recorded in the surveys. Independent from the flood duration and with the water reaching a maximum depth between 1 and 1.5 m, farmers estimated a 30% yield reduction with respect to the expected wheat yield. All the interviewed farmers cultivating winter wheat agreed on this loss value. Farmers cultivating alfalfa reported variable yield losses, ranging from 5 to 50% according to field location. Farmers with fields located near the levee breach reported huge losses, around 50% of their expected production, forcing them to reseed the crop in spring, while farmers with fields far from the breach reported yield losses between 10 and 20%.

4.2. Agricultural Losses Estimated through Models

Agricultural losses were evaluated at field scale for winter wheat and alfalfa. For winter wheat, the potential yield Y_{Pww}, i.e., the yield of winter wheat in the absence of the flood, retrieved from APSIM, WOFOST and AGRIDE-c is shown in Figure 9 together with the expected yield indicated by farmers during the interviews.

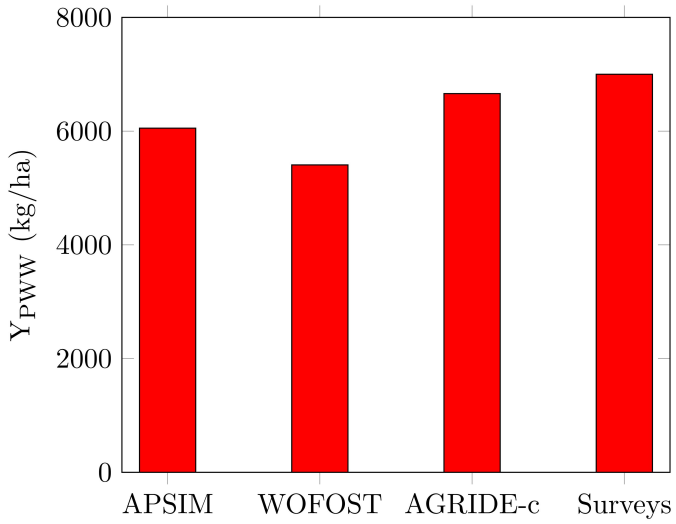

Figure 9. Winter wheat potential yield according to the crop models (APSIM and WOFOST), expert-based models (AGRIDE-c) and field surveys.

The reduced winter wheat yield, Y_{Rww}, depends on the amount of water that hits the crop. In APSIM and WOFOST the waterlogging effect causes a progressive yield reduction according to the water depth, while in AGRIDE-c the yield reduction depends on the flood duration, the crop vegetative stage and the water depth. At the time of the event, winter wheat was in its "three-leaf stage". The flood duration is reported in Figure 7. The crop damage, independent of the water depth, is 0 for a flood duration below four days, 25% for a flood duration of 5 days, 90% for a flood duration of 6 days and 100% for a flood duration longer than 6 days [61]. The flood duration over the winter wheat fields is reported in Appendix C Figure A2, while Figures A3–A5 show the damage estimation at the field scale obtained from the APSIM, WOFOST and AGRIDE-c in the two hazard scenarios (flood extent and water depth retrieved from FwDET and HEC-RAS, respectively, and flood duration retrieved as described in Section 3.1.3 from the AGRIDE-c).

For winter wheat, when the water depth and extent derived from FwDET were used to model the hazard, the overall yield loss amounted to 4.30% using AGRIDE-c, while it was 9.56% and 8.81% according to APSIM and WOFOST crop models, respectively (Table 5). When the water depth and extent were retrieved from HEC-RAS, the yield loss over all the winter wheat fields was 4.64, 9.81 and 10.25% according to AGRIDE-c, APSIM and

WOFOST, respectively (Table 5). All estimates were far from the 30% yield losses declared by the farmers (Figure 10).

Table 5. Winter wheat yield losses (a % of the potential yield) according to the crop models (APSIM and WOFOST) and expert-based model (AGRIDE-c), considering the different sources used to simulate the water depth, flood extent and flood duration. Values refer to the total number of winter wheat fields in the study area.

Hazard Source	AGRIDE-c	APSIM	WOFOST
FWDet	4.30	9.56	8.81
HEC-RAS	4.64	9.81	10.25

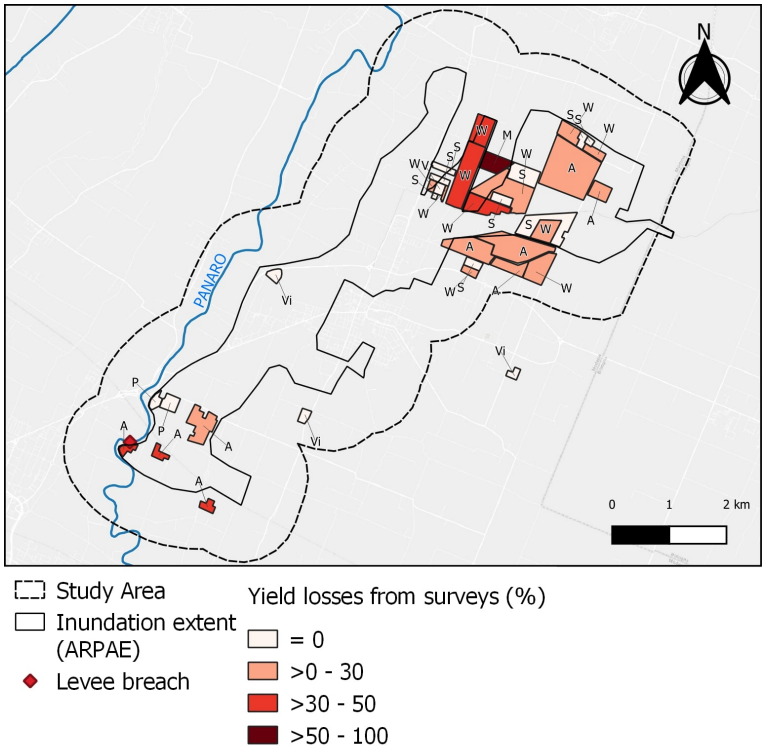

Figure 10. Crop yield losses declared by the farmers.

Alfalfa was at vegetative rest during December, thus the damage curves implemented in AGRIDE-c assume that the crop is unaffected by the flood in this period. As a consequence, the yield loss according to AGRIDE-c is always 0, independent of the water depth and flood duration.

The evaluation of the alfalfa yield loss was carried out with AGRIDE-c only. Even though crop models exist able to simulate alfalfa growth processes, such as APSIM-Lucerne [61] and APSIM Next-generation [62], they are unable to reproduce the effects of water excess. Studies evaluating waterlogging on forage at vegetative rest are still lacking [63]. In fact, although the scientific literature reports alfalfa to tolerate floods well, the interviewed farmers reported variable yield losses, ranging from 5 to 50% depending on field location (Figure 10).

5. Discussion

The first aim of the paper was to understand the differences in yield loss estimates retrieved using crop models and expert-based models, two conceptually different approaches. The use of crop models to assess crop yield losses due to flood is relatively new, since the mechanisms for waterlogging simulation have only recently been implemented in

models [53]. Thus, this study attempted to explore the possibility of applying crop models and expert-based models in combination with other information sources to estimate crop yield losses due to flood.

As is clearly seen in Table 5, for winter wheat APSIM and WOFOST (crop models) provided similar estimates of wheat losses if the same flood simulation source was considered. The two crop models, when run with the FwDET flood simulation, exhibited a difference of less than 1% in the final wheat yield loss estimations, with APSIM estimating slightly higher losses than WOFOST. When run with the HEC-RAS flood simulation, the difference in the loss estimates was again less than 1%, but APSIM estimated lower yield losses than WOFOST.

The difference between the losses evaluated by AGRIDE-c and the two crop models were significant. AGRIDE-c provided lower estimates of wheat yield loss than both the crop models. When the models were initialized with FwDET flood simulations, AGRIDE-c captured 4.30% of the wheat yield losses, about half the yield losses captured by the crop models (9.56% by APSIM and 8.81% by WOFOST). However, when the HEC-RAS flood simulation was used, AGRIDE-c captured 4.64% of the wheat losses, again around half the losses captured with the crop models.

The functions derived from the two crop models, APSIM and WOFOST, showed a similar behaviour. WOFOST reached a maximum yield reduction with a water depth of 25 cm, while APSIM showed a progressive decrease in yield until a water depth of 2 m (Figure 11). The difference is due to the mechanism used by the two models to simulate the effect of water excess on the crops. The difference between the yield reduction derived by the crop models and the one retrieved from AGRIDE-c is based on the fact that the two crop models base their yield loss estimations on water depth, while AGRIDE-c used flood duration. In fact, when wheat was in the "three-leaf stage", the crop damage in AGRIDE-c only depended flood duration and not water depth.

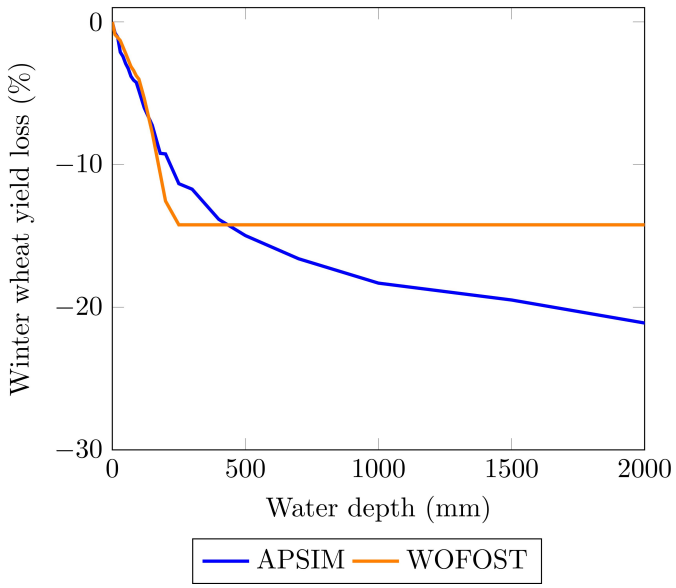

Figure 11. Relationship between the water depth and winter wheat yield reduction according to the crop models, APSIM and WOFOST.

A similar approach was not applied to evaluate alfalfa yield losses since the mechanisms to simulate the effect of water excess on forage are not yet implemented in the two crop models. Since models incorporating the effect of water excess on forage crops are still lacking, the expert-based model AGRIDE-c was useful to provide rough indications on possible damage to forage due to floods. The vulnerability of alfalfa to flood is supposed to be negligible when the crop is at vegetative rest.

Some studies support this statement, evidencing the tolerance of forage crops to waterlogging and their ability to recover from such a stress [64]. A study investigating the response of alfalfa to oxygen stress at different plant developmental stages found that yield losses were lower in plants subjected to high irradiance levels [65]; however, this study did not include the vegetative rest stage. Another research group found that the effect of flooding on reducing alfalfa yield losses depended on the crop growth stage, with floods happening in the early growth stages having a greater detrimental effect on the final crop yield [66].

Based on these considerations, the impact of flooding during the vegetative rest has not been deeply investigated in this study, assuming that the conditions taking place when the crop is at rest have no impact on plant development. The obtained results demonstrate the necessity of investigating the effect of flooding on crops at vegetative rest and perennial crops to understand whether, in extreme events, crops are able to recover from the stress or whether the yield losses remain significant in the following growing season.

Regarding the methodology adopted for flood hazard simulation, Table 5 shows that, when considering the same agricultural loss model, the difference between the obtained losses when the model is initialized with the FwDET or HEC-RAS flood simulations is negligible. In all three considered cases, the difference was less than 2%. Thus, two main considerations can be drawn from the present study, i.e., the agricultural loss estimation strongly depends on the agricultural loss model, and less detailed flood simulation methods can be applied without compromising the final loss estimate. In the present study, the average water depth over the flood extent obtained by FwDET and HEC-RAS was in good agreement, with the first indicating an average water depth of 0.42 m, and the second indicating 0.44 m even if significant differences persisted in the maximum values, with FwDET tending to overestimate the highest water depths compared to HEC-RAS (see Figure A6 in Appendix D). The general agreement of the water depths estimated using the two approaches could be a reason for the consistency of the yield losses estimated with APSIM and WOFOST. It should be highlighted that while the performance of HEC-RAS in simulating the flood parameters was compared to other models, such as LISFLOOD-FP [67], artificial neural network models [68] and SWE-FVM [69], FwDET's ability to reproduce water depth has never been compared with different hydraulic or hydrological models.

Furthermore, in the present study, the authors were able to collect additional information through surveying farmers and on-site inspections after the flood event. The combination of various information sources to assess flood damage has been traditionally performed to evaluate building damage. For example, [70] combined remote sensing images with object-based image analysis to estimate the number of damaged houses, while [71] exploited information retrieved from surveys carried on by the Italian National Fire Corps together with satellite images to evaluate residential and public building damage. Moreover, [72] developed vulnerability curves for 16 crops in Germany, taking into account crop sensitivity in different months of the year; however, they did not used of specific up-to-date data on the distribution of the crop types. However, the use of multiple information sources is uncommon in the assessment of flood damage to the agricultural sector. In fact, many studies have applied remote sensing techniques (see, for example, [73] reviewing 62 studies using remote sensing to evaluate crop losses due to flood), but only a couple of studies have combined various sources of information. For example, [74] used survey data to develop a generic crop vulnerability function and remote sensing techniques to map the flooded areas in a region of Bangladesh. The study did not consider different crop types or growth stages. Ref. [75] applied remote sensing images to evaluate the flood water depth and used vulnerability functions derived from expert knowledge to map rice damage due to flood in Southeast Asia. Both studies underlined the challenges in obtaining direct information on crop damage from farmers and combine them with model outputs.

Furthermore, in the present case considered the difficulties in exploiting additional information derived from surveys to validate the agricultural loss estimates and understand which agricultural loss model best reproduced the observations.

The retrieved questionnaires only enable a qualitative evaluation of the flood and agricultural loss models given their reduced number. From a qualitative point of view, it could be observed that farmers' declared losses always exceeded the modelled ones, with farmers declaring a 30% wheat yield reduction and between 5 and 50% alfalfa yield losses. These values are higher than modelled losses for both crops. For winter wheat, the modelled losses varied between 3 and 10% according to the different combinations of hazard and damage models used, while for alfalfa the modelled losses were always zero according to AGRIDE-c.

The higher losses declared by farmers could be linked with the fact that crop models are only able to reproduce part of the damage, i.e., damage due to waterlogging, while other mechanisms, such as water velocity, could contribute to the increased yield losses. Another explanation for the higher losses declared by farmers could be linked with the over-perception mechanism. Cognitive biases of this kind were found in [76], who highlighted a disconnect between the farmers' reports of losses and realized yields after extreme events. This topic deserves further attention since at present studies assessing farmers' perception of crop losses due to flood and extreme events are lacking. Cognitive biases could have led farmers to overestimate the severity of the flood and consequent damages. However, it is interesting to note that if the water depth would have been the one declared by the farmers, generally higher than the modelled one, the modelled winter wheat losses would have been more in line with the ones reported in the surveys. In fact, for a water depth of 1 m, as was declared by the farmers, the winter wheat yield losses at the field scale would have been around 20% according to APSIM and WOFOST. These values are more in line with the 30% yield losses reported by the farmers. Even if the authors managed to collect surveys from 30 fields, more interviews would have been necessary to obtain a complete picture of the event. An improvement in the strategies to involve farmers is necessary to collect adequate samples that can be used to validate the models, such as close collaboration with local authorities and farmer associations.

Moreover, the selected models take into account the water depth, the flood duration and the water speed but do not consider the effect of sediments. The amount of sediment left after a flood varies significantly from one case to another, mainly in relation to the inundation characteristics (sediment loads of the water) and water residence time. Typically, information on sediment deposits is limited to a rough estimation of the depth of the sediment, which may vary significantly from one location to another. To the best of our knowledge, no info on the nature of the sediment was available from field surveys and questionnaires. The impact on the crops is difficult to be estimated and might vary in relation to the strategies adopted by the farmers. The lack of detailed information on the sediment amount and characteristics, as well as the real impacts on crop productivity does not allow the inclusion of the sedimentary effects in the study. The topic is critical and deserves detailed investigations [17].

Finally, the results of this study have highlighted that even when different sources of information on both hazards and losses are available, the damage models presented in the scientific literature show limitations in reproducing crop yield losses due to flood as they fail to consider the effects of various damage mechanisms, such as flow velocity and a decrease in light availability due to plant submergence. The present work underlines the need for crop models capable of simulating flood-related losses for permanent forage crops, such as alfalfa, since the expert-based model AGRIDE-c assumes that the damage is null when alfalfa is at rest, while farmers reported losses between 5 and 50% of the expected yield. Furthermore, the unavailability of yield data at the field scale forced crop models calibration and validation to be performed using yield observations collected at the province scale, containing extensive variations. The use of yield data at the field scale could be interesting to perform a more accurate calibration of the crop models, thus obtaining a better representation of the yield losses due to flooding. The results also show that the improvement of the tools to model flood damage in agriculture is necessary to provide reliable damage estimations.

6. Conclusions

Agriculture is traditionally highly vulnerable to natural hazards, and floods play a crucial role in lowering crop productivity. Understanding the effect of floods in reducing crop productivity is of mandatory importance to develop modelling tools that can provide information on yield losses in case of an extreme event. The choice of the modelling tools to reproduce both the agricultural losses and the flood features influences the final results.

This study aimed to (1) understand the differences in the yield loss estimation retrieved using two conceptually different approaches to model agricultural losses (crop models and expert-based models); (2) assess how the crop yield loss estimations change in response to different methodologies to simulate water depth, flood extent and duration; (3) investigate the challenges and future developments in flood crop damage based on the results obtained for a past events for which multi-source information was available. Two crop models (APSIM and WOFOST) and the expert-based model AGRIDE-c were applied to evaluate the agricultural losses, while a hydraulic model (HEC-RAS) and a flood feature estimation tool from remote sensing (FwDET) were tested to understand the sensitivity of the agricultural loss models to flood hazard simulation. Finally, surveys and on-site inspections performed by the authors were evaluated as possible additional sources of information to validate the models.

The main findings of the study are the following:

- The two crop models, APSIM and WOFOST, provided similar estimates for wheat loss when initialized with the same flood simulation; contrarily, the expert-based model provided lower yield losses compared to the crop models.
- The choice of the hazard simulation method did not significantly influence the agricultural loss estimation. When the same loss model was applied, the difference between the agricultural loss estimates obtained using HEC-RAS or FwDET to simulate the average water depth was less than 2%.
- The availability of additional information, such as on-site inspections and surveys on the flood features (extent, duration and water depth) and agricultural losses is useful to provide a qualitative picture of the event and its consequences. However, it is still difficult to use such information to validate the agricultural loss estimates provided by the models. When involvement of farmer associations or local authorities is important to collect a sufficient number of surveys on an event.

The research has shown that including different types of information into evaluate agricultural losses due to flood is still challenging, given the shortcomings still present in the existing crop damage estimation models.

Author Contributions: Conceptualization: B.M., M.A. and I.B.; formal analysis: B.M. and A.M.; investigation and visualisation: R.G. and N.P.; Supervision: A.D., A.C., B.B. and M.L.V.M.; writing—original draft: B.M., R.G., M.A. and I.B. All authors have read and agreed to the published version of the manuscript.

Funding: This work was supported by the Italian Ministry of Education, within the framework of the project Dipartimenti di Eccellenza 2023–2027 (L.11/12/2016 n.232) at IUSS Pavia, by the Regione Lombardia within the framework of the project IUSS Data Center (DGR n.XI/3776/2020) and, the project MOVIDA (Metodologie e Applicazioni per l'aggiornamento delle mappe di danno alluvionale relativamente alla revisione del PGRA) that was funded by the Po River District Authority and co-funded by the consortium of universities and research centres involved in the project: Politecnico di Milano, University School for Advanced Studies (IUSS) Pavia, University of Florence, University of Turin, University of Bologna, University of Ferrara, University of Brescia, University of l'Aquila, and the National Research Council (CNR) and by the Autoritá di Bacino del Distretto Idrografico della Sicilia (grant no. F62G16000000001) "Linea di intervento L1 Bilancio idrico—Studi per l'analisi delle pressioni idrologiche—la gestione sostenibile delle risorse idriche secondo la direttiva 2000/60 e per la governance in regime di siccitá e per l' adattamento ai cambiamenti climatici."

Data Availability Statement: Not applicable.

Conflicts of Interest: The authors declare no conflict of interest.

Appendix A

Appendix A reports the English translation of the survey proposed to the interviewed farmers. The original survey was written in Italian. The survey was divided into two sections, Section A and Section B.

Section A: General information. Please indicate:

1. Name of the farm, email and phone contact.
2. Closest address to the position of the considered field. Please also fill in the attached maps identifying the cultivated areas affected by the flood and the types of cultivation.

Section B: Farm exposure. Please indicate:

1. The crop type grown in the considered field.
2. Size of the field.
3. Years of operation.
4. Average annual yield.
5. Maximum annual yield.
6. Phenological state of the crop at the time of the flood (6 December 2020).
7. How much was spent on cultivation during the agricultural season before the flood.
8. Which of these operations had already been carried out before the flood and how much was spent (in Euros) for each of them? (Ploughing, harrowing, pre-sowing weeding, sowing, weeding, fertilization, irrigation, harvesting, planting, pruning, soil preparation, pesticide spreading, and fungicide spreading).

Appendix B

Appendix B provides further details on crop model calibration. Observed yield data were extracted from the agricultural statistics database of the Italian National Institute of Statistics [57]. Yield data for the Modena province were used for model calibration (2006–2014) and validation (2015–2020).

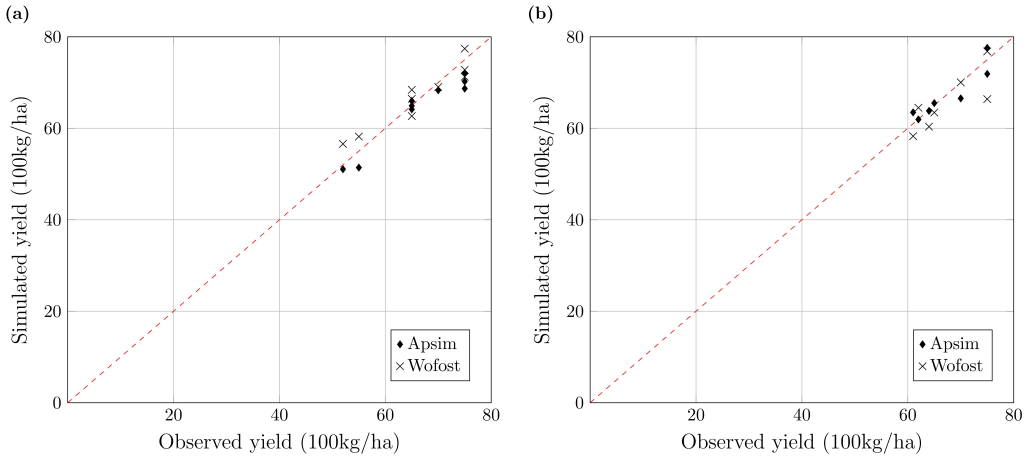

Figure A1. Crop model calibration (**a**) and validation (**b**).

Since the observed yield data are only available at the province level, weather data at the province level were retrieved from the E-OBS database v.25e (daily rainfall, solar radiation, minimum, maximum and average temperature and wind speed). E-OBS is a daily gridded land-only observational dataset over Europe with a spatial resolution of 0.1° [77]. Agricultural areas of the Modena province were extracted from the Corine Land Cover map [44]. The soil texture of the agricultural areas of the Modena province was derived from the SoilGrids dataset [56]. Based on the SoilGrids dataset, the soil type used in both crop models was a loam soil (generic loam soil in APSIM and a very fine texture in WOFOST). In both models the wheat sowing window is supposed to be from 20 to

31 October. Nitrogen fertilizer is applied at sowing and flowering. The total amount of nitrogen fertilizer was 150 kg/ha. In APSIM, the sowing density was fixed at 350 plants/m^2, the sowing depth to 50 mm and the row spacing to 250 mm. The model calibration and validation results were satisfactory (Figure A1). In particular, the Pearson correlation coefficient for model calibration was 0.92 and 0.90 for APSIM and WOFOST, respectively, while the Pearson correlation coefficient for model validation was 0.85 and 0.71 for APSIM and WOFOST, respectively.

Appendix C

Appendix C reports the maps showing the flood duration in the winter wheat fields and the wheat damage estimations performed at the field level. Figure A2 shows the flood duration over the winter wheat fields. Figure A3 shows a comparison between the damage estimation performed with APSIM using (a) the flood extent and water depth derived from FwDET; (b) the flood extent and water depth derived from HEC-RAS. Figure A4 shows a comparison between the damage estimation performed with WOFOST using (a)the flood extent and water depth derived from FwDET; (b) the flood extent and water depth derived from HEC-RAS. Figure A5 shows a comparison between the damage estimation performed with AGRIDE-c using (a) the flood extent and water depth derived from FwDET; (b) the flood extent and water depth derived from HEC-RAS.

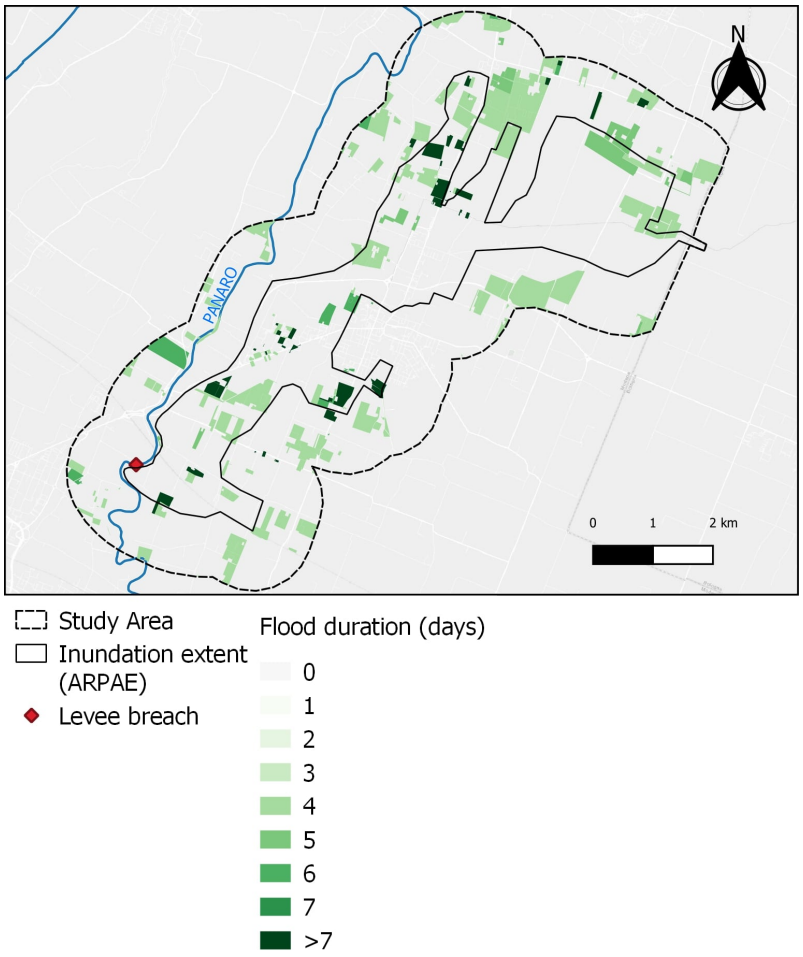

Figure A2. Flood duration in the winter wheat fields determined by the sources listed in Table 3.

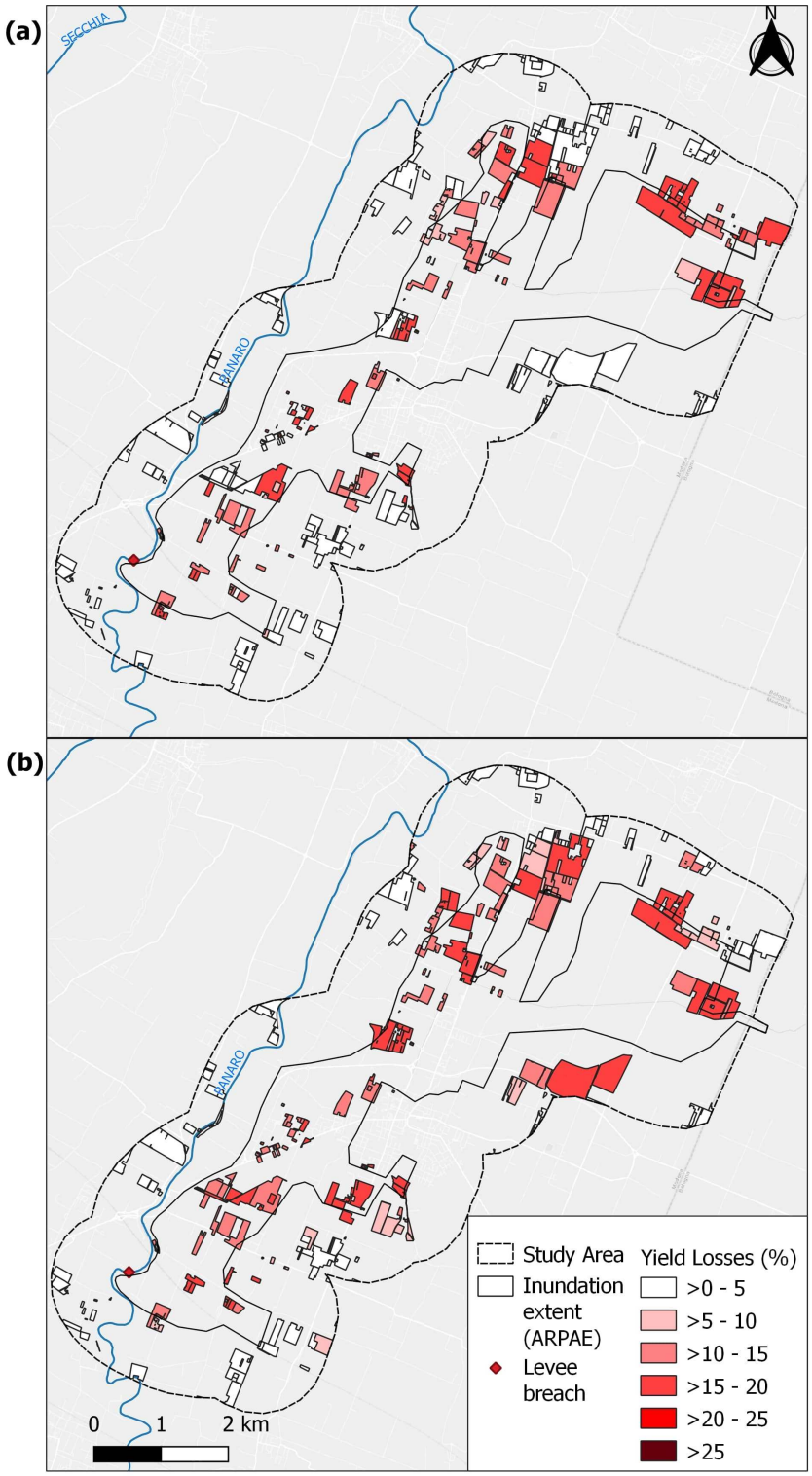

Figure A3. Comparison between the damage estimation performed with APSIM using (**a**) the flood extent and water depth derived from FwDET; (**b**) the flood extent and water depth derived from HEC-RAS.

Figure A4. Comparison between the damage estimation performed with WOFOST using (**a**) the flood ex-tent and water depth derived from FwDET; (**b**) the flood extent and water depth derived from HEC-RAS.

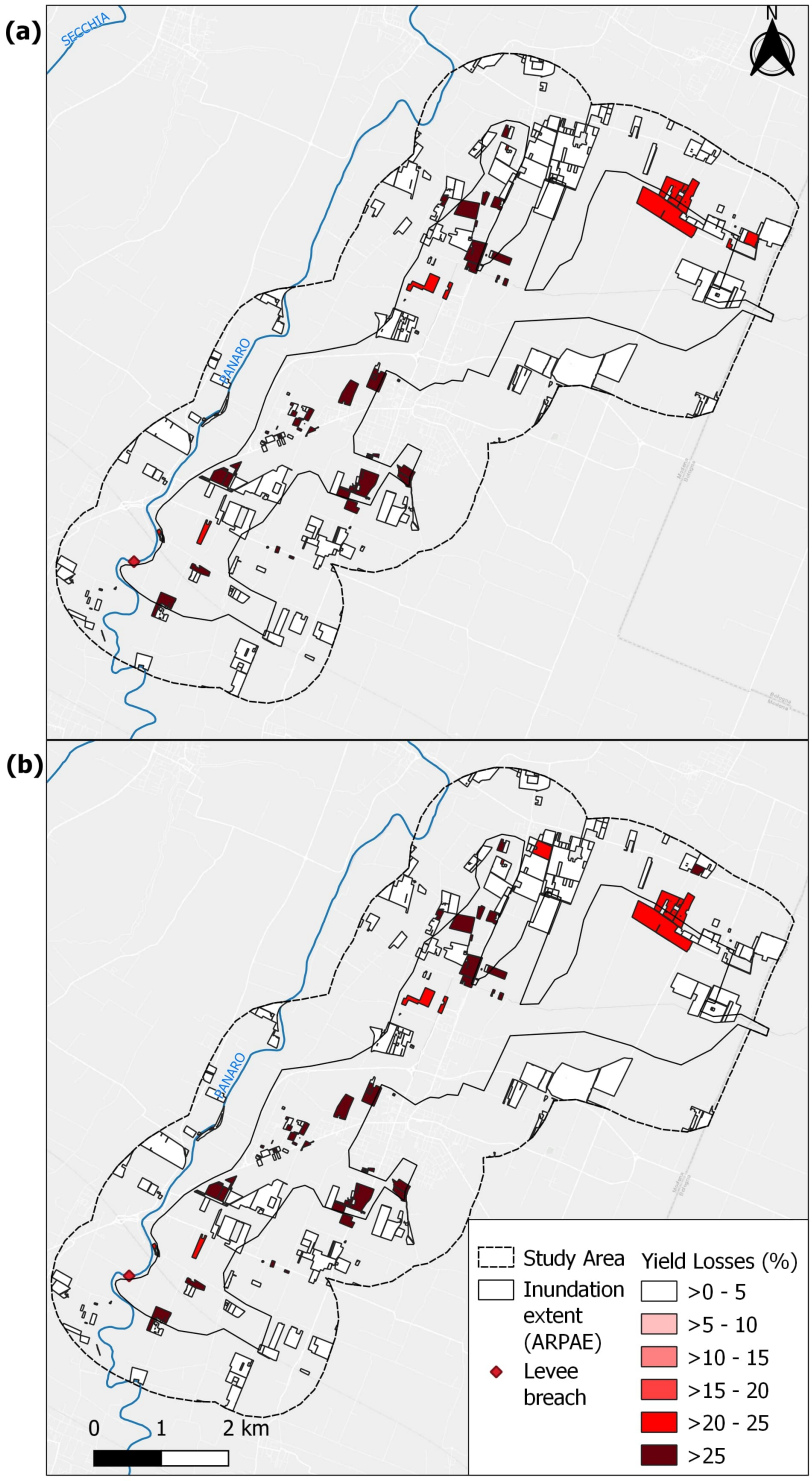

Figure A5. Comparison between the damage estimation performed with AGRIDE-c using (**a**) the flood ex-tent and water depth derived from FwDET; (**b**) the flood extent and water depth derived from HEC-RAS.

Appendix D

Appendix D shows the differences between the HEC-RAS and FwDET water depth estimations of the flooded fields.

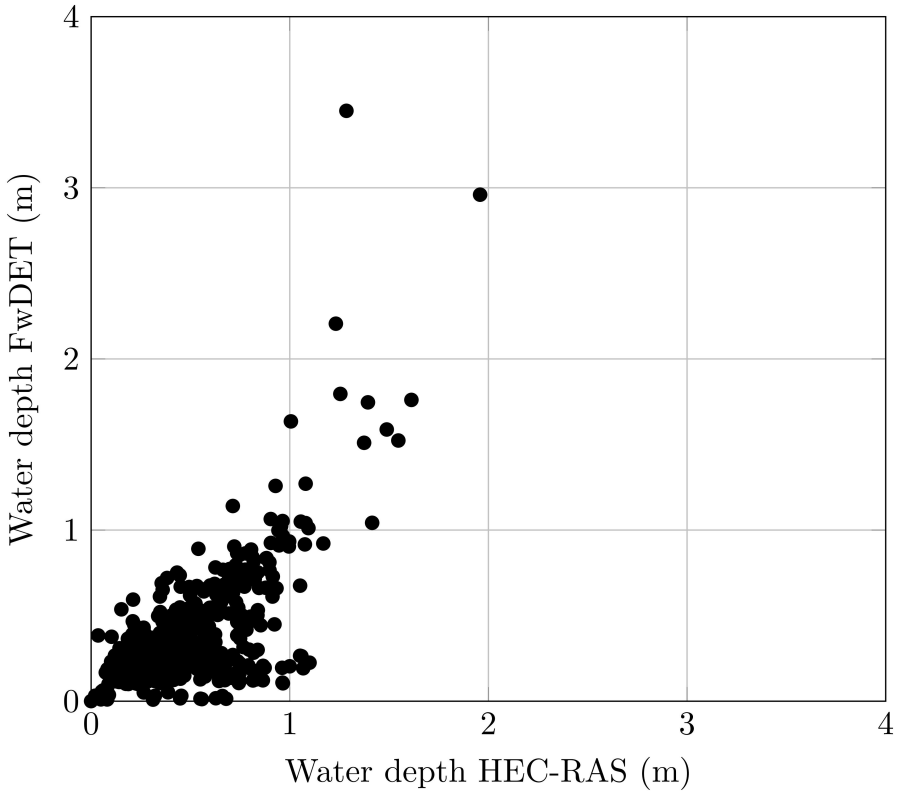

Figure A6. Differences in the HEC-RAS and FwDET water depth estimations of the flooded fields.

References

1. FAO. *The Impact of Disasters and Crises on Agriculture and Food Security: 2021*; Technical Report; FAO: Rome, Italy, 2021. [CrossRef]
2. FAO. *Impact of Natural Hazards and Disasters on Agriculture and Food Security and Nutrition*; Technical Report; FAO: Rome, Italy, 2015.
3. Merz, B.; Kreibich, H.; Schwarze, R.; Thieken, A. Review article "assessment of economic flood damage". *Nat. Hazards Earth Syst. Sci.* **2010**, *10*, 1697–1724. [CrossRef]
4. Brémond, P.; Grelot, F. Review Article: Economic evaluation of flood damage to agriculture—Review and analysis of existing methods. *Nat. Hazards Earth Syst. Sci.* **2013**, *13*, 2493–2512. [CrossRef]
5. Lesk, C.; Rowhani, P.; Ramankutty, N. Influence of extreme weather disasters on global crop production. *Nature* **2016**, *529*, 84–87. [CrossRef] [PubMed]
6. Shrestha, B.; Okazumi, T.; Miyamoto, M.; Sawano, H. Flood damage assessment in the Pampanga river basin of the Philippines. *J. Flood Risk Manag.* **2016**, *9*, 355–369. [CrossRef]
7. Klaus, S.; Kreibich, H.; Merz, B.; Kuhlmann, B.; Schröter, K. Large-scale, seasonal flood risk analysis for agricultural crops in Germany. *Environ. Earth Sci.* **2016**, *75*, 1289. [CrossRef]
8. Monteleone, B.; Borzí, I.; Bonaccorso, B.; Martina, M. Quantifying crop vulnerability to weather-related extreme events and climate change through vulnerability curves. *Nat. Hazards* **2023**, *116*, 2761–2796. [CrossRef]
9. Shrestha, B.B.; Sawano, H.; Ohara, M.; Nagumo, N. Improvement in flood disaster damage assessment using highly accurate IfSAR DEM. *J. Disaster Res.* **2016**, *11*, 1137–1149. [CrossRef]
10. Shrestha, B.B.; Kawasaki, A.; Zin, W.W. Development of flood damage functions for agricultural crops and their applicability in regions of Asia. *J. Hydrol. Reg. Stud.* **2021**, *36*, 100872. [CrossRef]
11. Kwak, Y.; Shrestha, B.B.; Yorozuya, A.; Sawano, H. Rapid Damage Assessment of Rice Crop After Large-Scale Flood in the Cambodian Floodplain Using Temporal Spatial Data. *IEEE J. Sel. Top. Appl. Earth Obs. Remote Sens.* **2015**, *8*, 3700–3709. [CrossRef]
12. Vozinaki, A.E.K.; Karatzas, G.P.; Sibetheros, I.A.; Varouchakis, E.A. An agricultural flash flood loss estimation methodology: The case study of the Koiliaris basin (Greece), February 2003 flood. *Nat. Hazards* **2015**, *79*, 899–920. [CrossRef]
13. Li, K.; Wu, S.; Dai, E.; Xu, Z. Flood loss analysis and quantitative risk assessment in China. *Nat. Hazards* **2012**, *63*, 737–760. [CrossRef]
14. Ming, X.; Xu, W.; Li, Y.; Du, J.; Liu, B.; Shi, P. Quantitative multi-hazard risk assessment with vulnerability surface and hazard joint return period. *Stoch. Environ. Res. Risk Assess.* **2015**, *29*, 35–44. [CrossRef]
15. Ganji, Z.; Shokoohi, A.; Samani, J.M.V. Developing an agricultural flood loss estimation function (case study: Rice). *Nat. Hazards* **2012**, *64*, 405–419. [CrossRef]

16. Brémond, P.; Agenais, A.L.; Grelot, F.; Richert, C. Process-based flood damage modelling relying on expert knowledge: A methodological contribution applied to the agricultural sector. *Nat. Hazards Earth Syst. Sci.* **2022**, *22*, 3385–3412. [CrossRef]
17. Molinari, D.; Rita Scorzini, A.; Gallazzi, A.; Ballio, F. AGRIDE-c, a conceptual model for the estimation of flood damage to crops: Development and implementation. *Nat. Hazards Earth Syst. Sci.* **2019**, *19*, 2565–2582. [CrossRef]
18. Förster, S.; Kuhlmann, B.; Lindenschmidt, K.E.; Bronstert, A. Assessing flood risk for a rural detention area. *Nat. Hazards Earth Syst. Sci.* **2008**, *8*, 311–322. [CrossRef]
19. Keating, B.; Carberry, P.; Hammer, G.; Probert, M.; Robertson, M.; Holzworth, D.; Huth, N.; Hargreaves, J.; Meinke, H.; Hochman, Z.; et al. An overview of APSIM, a model designed for farming systems simulation. *Eur. J. Agron.* **2003**, *18*, 267–288. [CrossRef]
20. Pasley, H.R.; Huber, I.; Castellano, M.J.; Archontoulis, S.V. Modeling Flood-Induced Stress in Soybeans. *Front. Plant Sci.* **2020**, *11*, 62. [CrossRef]
21. Kaur, G.; Singh, G.; Motavalli, P.P.; Nelson, K.A.; Orlowski, J.M.; Golden, B.R. Impacts and management strategies for crop production in waterlogged or flooded soils: A review. *Agron. J.* **2020**, *112*, 1475–1501. [CrossRef]
22. Apel, H.; Aronica, G.T.; Kreibich, H.; Thieken, A.H. Flood risk analyses—How detailed do we need to be? *Nat. Hazards* **2009**, *49*, 79–98. [CrossRef]
23. Magnini, A.; Lombardi, M.; Persiano, S.; Tirri, A.; Lo Conti, F.; Castellarin, A. Machine-learning blends of geomorphic descriptors: Value and limitations for flood hazard assessment across large floodplains. *Nat. Hazards Earth Syst. Sci.* **2022**, *22*, 1469–1486. [CrossRef]
24. Schumann, G.J.P.; Domeneghetti, A. Exploiting the proliferation of current and future satellite observations of rivers. *Hydrol. Process.* **2016**, *30*, 2891–2896. [CrossRef]
25. Tavares da Costa, R.; Zanardo, S.; Bagli, S.; Hilberts, A.G.J.; Manfreda, S.; Samela, C.; Castellarin, A. Predictive Modeling of Envelope Flood Extents Using Geomorphic and Climatic Hydrologic Catchment Characteristics. *Water Resour. Res.* **2020**, *56*, e2019WR026453. [CrossRef]
26. Alfieri, L.; Cohen, S.; Galantowicz, J.; Schumann, G.J.P.; Trigg, M.A.; Zsoter, E.; Prudhomme, C.; Kruczkiewicz, A.; Coughlan de Perez, E.; Flamig, Z.; et al. A global network for operational flood risk reduction. *Environ. Sci. Policy* **2018**, *84*, 149–158. [CrossRef]
27. Sampson, C.C.; Smith, A.M.; Bates, P.D.; Neal, J.C.; Alfieri, L.; Freer, J.E. A high-resolution global flood hazard model. *Water Resour. Res.* **2015**, *51*, 7358–7381. [CrossRef]
28. Arosio, M.; Cesarini, L.; Martina, M.L.V. Assessment of the Disaster Resilience of Complex Systems: The Case of the Flood Resilience of a Densely Populated City. *Water* **2021**, *13*, 2830. [CrossRef]
29. Cesarini, L.; Figueiredo, R.; Monteleone, B.; Martina, M.L.V. The potential of machine learning for weather index insurance. *Nat. Hazards Earth Syst. Sci.* **2021**, *21*, 2379–2405. [CrossRef]
30. Cohen, S.; Raney, A.; Munasinghe, D.; Loftis, J.D.; Molthan, A.; Bell, J.; Rogers, L.; Galantowicz, J.; Brakenridge, G.R.; Kettner, A.J.; et al. The Floodwater Depth Estimation Tool (FwDET v2.0) for improved remote sensing analysis of coastal flooding. *Nat. Hazards Earth Syst. Sci.* **2019**, *19*, 2053–2065. [CrossRef]
31. Nguyen, N.Y.; Ichikawa, Y.; Ishidaira, H. Estimation of inundation depth using flood extent information and hydrodynamic simulations. *Hydrol. Res. Lett.* **2016**, *10*, 39–44. [CrossRef]
32. Scorzini, A.R.; Di Bacco, M.; Manella, G. Regional flood risk analysis for agricultural crops: Insights from the implementation of AGRIDE-c in central Italy. *Int. J. Disaster Risk Reduct.* **2021**, *53*, 101999. [CrossRef]
33. Celano, M.; Foraci, R.; Selvini, A.; Biolchi, L.; Valentini, A.; Unguendoli, S.; Baroni, C.; Daniele, G.; Pizziolo, M. Rapporto dell'Evento Meteorologico, delle Piene e delle Frane Occorsi. 2021. Available online: https://www.arpae.it/it/temi-ambientali/meteo/report-meteo/rapporti-post-evento/rapporto_meteo_idro_geo_20201204-08-1.pdf/@@display-file/file/Rapporto_meteo_idro_geo_20201204-08.pdf (accessed on 15 May 2023).
34. Consorzio di Bonifica della Burana. Rotta Fiume Panaro Domenica 6 Dicembre 2020. 2020. Available online: https://www.consorzioburana.it/upload/burana/gestionedocumentale/ROTTAPANARO6dicembre2020_784_15341.pdf (accessed on 15 May 2023).
35. Direzione Generale Agricoltura Caccia e Pesca Disciplinare di Produzione Integrata—Norme Generali; Technical Report. 2022. Available online: https://agricoltura.regione.emilia-romagna.it/produzioni-agroalimentari/temi/bio-agro-climambiente/agricoltura-integrata/disciplinari-produzione-integrata-vegetale/Collezione-dpi/dpi_2022/norme-generali-2022 (accessed on 15 May 2023).
36. Regione Emilia-Romagna. Geoportale. 2022. Available online: https://geoportale.regione.emilia-romagna.it/ (accessed on 22 July 2022).
37. Regione Emilia-Romagna. Disciplinari di Produzione Integrata 2021—Norme Tecniche di Coltura, Colture Erbacee, Frumento Tenero e Duro. 2021. Available online: https://agricoltura.regione.emilia-romagna.it/produzioni-agroalimentari/temi/bio-agro-climambiente/agricoltura-integrata/disciplinari-produzione-integrata-vegetale/Collezione-dpi/dpi_2022/erbacee-2021 (accessed on 15 May 2023).
38. Regione Emilia-Romagna. Disciplinari di Produzione Integrata 2021—Norme Tecniche di Coltura, Colture Erbacee, Sorgo. 2021. Available online: https://agricoltura.regione.emilia-romagna.it/produzioni-agroalimentari/temi/bio-agro-climambiente/agricoltura-integrata/disciplinari-produzione-integrata-vegetale/Collezione-dpi/dpi_2022/norme-tecniche-di-coltura-2022 (accessed on 15 May 2023).

39. Regione Emilia-Romagna. Disciplinari di Produzione Integrata 2021—Norme Tecniche di Coltura, Colture Erbacee, Mais. 2021. Available online: https://agricoltura.regione.emilia-romagna.it/produzioni-agroalimentari/temi/bio-agro-climambiente/agricoltura-integrata/disciplinari-produzione-integrata-vegetale/Collezione-dpi/dpi_2022/norme-tecniche-di-coltura-2022 (accessed on 15 May 2023).
40. Regione Emilia-Romagna. Regione Emilia-Romagna—Disciplinari di Produzione Integrata 2017—Norme Tecniche di Coltura, Colture Erbacee, Erba Medica. 2017. Available online: https://agricoltura.regione.emilia-romagna.it/produzioni-agroalimentari/temi/bio-agro-climambiente/agricoltura-integrata/disciplinari-produzione-integrata-vegetale/Collezione-dpi/dpi_2022/norme-tecniche-di-coltura-2022 (accessed on 15 May 2023).
41. USACE. *HEC-RAS River Analysis System User's Manual Version 6.0*; USACE: Washington, DC, USA, 2021.
42. de Wit, A.; Boogaard, H.; Fumagalli, D.; Janssen, S.; Knapen, R.; van Kraalingen, D.; Supit, I.; van der Wijngaart, R.; van Diepen, K. 25 Years of the WOFOST Cropping Systems Model. *Agric. Syst.* **2019**, *168*, 154–167. [CrossRef]
43. US Army Corps of Engineers. *Hydraulic Reference Manual*; US Army Corps of Engineers: Washington, DC, USA, 2001.
44. European Environment Agency (EEA). 2018 Corine Land Cover. 2021. Available online: https://land.copernicus.eu/pan-european/corine-land-cover (accessed on 10 February 2023).
45. Menduni, G.; Cocchi, R.; Manselli, L.; Simonini, P. Commissione Tecnico-Scientifica per la Valutazione delle Cause all'Origine della Rotta Arginale Lungo il Fiume Panaro in Località Gaggio di Castelfranco Emilia—Relazione di Dettaglio. 2021. Available online: https://ambiente.regione.emilia-romagna.it/it/notizie/allegati/allegati-2021/prot__02-03-2021_0177836-allegato-ndeg-1-relazione_di_dettaglio_sgn_-1-_timbrato.pdf (accessed on 15 May 2023).
46. Italian Space Agency. 2021. Available online: https://www.asi.it/en/the-agency/ (accessed on 10 February 2023).
47. ARPAE. Dati ARPAE—Emilia Romagna. Available online: https://dati.arpae.it/ (accessed on 22 November 2022).
48. Provincia di Modena. Nonantola—Riaperta la Sp 14 Fino a La Grande. Resta Chiuso Tratto della Sp 255 Nonantolana. 2020. Available online: https://www.provincia.modena.it/ext/1/77229/comunicato_stampa/nonantola-riaperta-la-sp-14-fino-a-la-grande-resta-chiuso-tratto-della-sp-255-nonantolana/ (accessed on 1 May 2023).
49. Provincia di Modena. Nonantola, Riaperto il Sottopasso sulla Provinciale 14. Esercito al Lavoro Sempre sulla Sp 14 a "la Grande". 2020. Available online: https://www.provincia.modena.it/ext/1/77246/comunicato_stampa/nonantola-riaperto-il-sottopasso-sulla-provinciale-14-esercito-al-lavoro-sempre-sulla-sp-14-a-la-grande/ (accessed on 1 May 2023).
50. Modena Today. Nonantola, Altri Cento Interventi della Protezione Civile. Esercito e Pompieri Rientrano. 2020. Available online: https://www.modenatoday.it/attualita/interventi-pulizia-nonantola-10-dicembre-2020.html (accessed on 1 May 2023).
51. Redazione Sul Panaro. Esondazione del Panaro a Nonantola, Aggiornamento di Venerdì 11 Dicembre. 2020. Available online: https://www.sulpanaro.net/2020/12/esondazione-del-panaro-a-nonantola-aggiornamento-di-venerdi-11-dicembre/ (accessed on 1 May 2023).
52. Copernicus Emergency Management Service. EMSR487: Flood in Emilia-Romagna Region, Italy, Grading Map, Monitoring 1. 2020. Available online: https://emergency.copernicus.eu/mapping/system/files/components/EMSR487_AOI02_GRA_PRODUCT_r1_RTP01_v1.pdf (accessed on 1 May 2023).
53. Liu, K.; Harrison, M.T.; Shabala, S.; Meinke, H.; Ahmed, I.; Zhang, Y.; Tian, X.; Zhou, M. The State of the Art in Modeling Waterlogging Impacts on Plants: What Do We Know and What Do We Need to Know. *Earth's Future* **2020**, *8*, e2020EF001801. [CrossRef]
54. Zheng, B.; Chenu, K.; Doherty, A.; Chapman, S. The APSIM-Wheat Module (7.5 R3008). 2015. Available online: https://www.apsim.info/wp-content/uploads/2019/09/WheatDocumentation.pdf (accessed on 15 May 2023).
55. Soil Science Division Staff. *Soil Survey Manual, USDA*; Number 18; USDA: Washington, DC, USA, 2017; p. 639.
56. Hengl, T.; Mendes de Jesus, J.; Heuvelink, G.B.M.; Ruiperez Gonzalez, M.; Kilibarda, M.; Blagotić, A.; Shangguan, W.; Wright, M.N.; Geng, X.; Bauer-Marschallinger, B.; et al. SoilGrids250m: Global gridded soil information based on machine learning. *PLoS ONE* **2017**, *12*, e0169748. [CrossRef] [PubMed]
57. Italian National Institute of Statistics. *I.stat* Italian National Institute of Statistics: Rome, Italy, 2021.
58. Monteleone, B.; Borzí, I.; Bonaccorso, B.; Martina, M. Developing stage-specific drought vulnerability curves for maize: The case study of the Po River basin. *Agric. Water Manag.* **2022**, *269*, 107713. [CrossRef]
59. Molinari, D.; Scorzini, A.R.; Gallazzi, A.; Ballio, F. AGRIDE-c simulator. *Mendeley Data* **2019**. [CrossRef]
60. Koenig, T.; Bruce, J.; O'Connor, J.; McGee, B.; Holmes, R.R., Jr.; Hollins, R.; Forbes, B.; Kohn, M.; Schellekens, M.; Martin, Z.; et al. *Identifying and Preserving High-Water Mark Data: U.S. Geological Survey Techniques and Methods*; Technical Report; USGS: Reston, VA, USA, 2016. [CrossRef]
61. Moot, D.; Hargreaves, J.; Brown, H.; Teixeira, E. Calibration of the APSIM-Lucerne model for "Grasslands Kaituna" lucerne crops grown in New Zealand. *N. Z. J. Agric. Res.* **2015**, *58*, 190–202. [CrossRef]
62. Yang, X.; Brown, H.E.; Teixeira, E.I.; Moot, D.J. Development of a lucerne model in APSIM next generation: 1 phenology and morphology of genotypes with different fall dormancies. *Eur. J. Agron.* **2021**, *130*, 126372. [CrossRef]
63. Striker, G.G.; Colmer, T.D. Flooding tolerance of forage legumes. *J. Exp. Bot.* **2016**, *68*, erw239. [CrossRef]
64. Ploschuk, R.A.; Grimoldi, A.A.; Ploschuk, E.L.; Striker, G.G. Growth during recovery evidences the waterlogging tolerance of forage grasses. *Crop. Pasture Sci.* **2017**, *68*, 574–582. [CrossRef]
65. Barta, A.L.; Sulc, R.M. Interaction between waterlogging injury and irradiance level in alfalfa. *Crop. Sci.* **2002**, *42*, 1529–1534. [CrossRef]

66. Teutsch, C.D.; Sulc, R.M. Influence of seedling growth stage on flooding injury in alfalfa. *Agron. J.* **1997**, *89*, 970–975. [CrossRef]
67. Shustikova, I.; Domeneghetti, A.; Neal, J.C.; Bates, P.; Castellarin, A. Comparing 2D capabilities of HEC-RAS and LISFLOOD-FP on complex topography. *Hydrol. Sci. J.* **2019**, *64*, 1769–1782. [CrossRef]
68. Tamiru, H.; Dinka, M.O. Application of ANN and HEC-RAS model for flood inundation mapping in lower Baro Akobo River Basin, Ethiopia. *J. Hydrol. Reg. Stud.* **2021**, *36*, 100855. [CrossRef]
69. Costabile, P.; Costanzo, C.; Ferraro, D.; Macchione, F.; Petaccia, G. Performances of the new HEC-RAS version 5 for 2-D hydrodynamic-based rainfall-runoff simulations at basin scale: Comparison with a state-of-the art model. *Water* **2020**, *12*, 2326. [CrossRef]
70. Jiménez-Jiménez, S.I.; Ojeda-Bustamante, W.; Ontiveros-Capurata, R.E.; Marcial-Pablo, M.d.J. Rapid urban flood damage assessment using high resolution remote sensing data and an object-based approach. *Geomat. Nat. Hazards Risk* **2020**, *11*, 906–927. [CrossRef]
71. Manselli, L.; Molinari, D.; Pogliani, A.; Zambrini, F.; Menduni, G. Improvements and Operational Application of a Zero-Order Quick Assessment Model for Flood Damage: A Case Study in Italy. *Water* **2022**, *14*, 373. [CrossRef]
72. GIS-based estimation of flood damage to arable crops. *AGIT J. Angew. Geoinform.* **2020**, *6*, 183–194.
73. Rahman, M.S.; Di, L. A Systematic Review on Case Studies of Remote-Sensing-Based Flood Crop Loss Assessment. *Agriculture* **2020**, *10*, 131. [CrossRef]
74. Bhuiyan, S.R.; Al Baky, A. Digital elevation based flood hazard and vulnerability study at various return periods in Sirajganj Sadar Upazila, Bangladesh. *Int. J. Disatsre Risk Reduct.* **2014**, *10*, 48–58. [CrossRef]
75. Shrestha, B.B.; Perera, E.D.P.; Kudo, S.; Miyamoto, M.; Yamazaki, Y.; Daisuke, K.; Sawano, H.; Sayama, T.; Magome, J.; Hasegawa, A.; et al. Assessing flood disaster impacts in agriculture under climate change in the river basins of Southeast Asia. *Nat. Hazards* **2019**, *97*, 157–192. [CrossRef]
76. Markhof, Y.; Randolph, P.; Ponzini, G. Loss(t) in Translation? Measuring Disaster Crop Losses in Surveys. 2022. Available online: https://blogs.worldbank.org/developmenttalk/losst-translation-measuring-disaster-crop-losses-surveys (accessed 5 May 2023).
77. Cornes, R.C.; van der Schrier, G.; van den Besselaar, E.J.; Jones, P.D. An Ensemble Version of the E-OBS Temperature and Precipitation Data Sets. *J. Geophys. Res. Atmos.* **2018**, *123*, 9391–9409. [CrossRef]